Period-Doubling Bifurcation in an Array of Coupled Stochastically Excitable Elements Subjected to Global Periodic Forcing

Xiaohua Cui,[1,2] Robert J. Rovetti,[3] Ling Yang,[4] Alan Garfinkel,[1,5] James N. Weiss,[5,6] and Zhilin Qu[5,*]

[1]*Department of Physiological Science, University of California, Los Angeles, California 90095, USA*
[2]*Department of Physics, Beijing Normal University, Beijing 100875, P.R. China*
[3]*Department of Mathematics, Loyola Marymount University, Los Angeles, California 90045, USA*
[4]*Center for Systems Biology, Shuzhou University, Jiangsu 215006, P.R. China*
[5]*Department of Medicine (Cardiology), David Geffen School of Medicine, University of California, Los Angeles, California 90095, USA*
[6]*Department of Physiology, David Geffen School of Medicine, University of California, Los Angeles, California 90095, USA*

(Received 23 March 2009; published 22 July 2009)

The collective behaviors of coupled, stochastically excitable elements subjected to global periodic forcing are investigated numerically and analytically. We show that the whole system undergoes a period-doubling bifurcation as the driving period decreases, while the individual elements still exhibit random excitations. Using a mean-field representation, we show that this macroscopic bifurcation behavior is caused by interactions between the random excitation, the refractory period, and recruitment (spatial cooperativity) of the excitable elements.

DOI: 10.1103/PhysRevLett.103.044102 PACS numbers: 05.45.Xt, 64.60.Ht, 89.75.−k

Collective behaviors that arise from coupled oscillators have been a long-term interest in nonlinear dynamics [1–3]. The most widely studied model is the Kuramoto model, in which periodic oscillators with randomly distributed frequencies are globally coupled [4,5]. These coupled oscillators can be synchronized to a single frequency, resulting in periodic behaviors and other complex non-random dynamics. In a recent study [6], a new type of coupled oscillator system has been developed, in which the individual oscillators are described by a three-state model whose period varies randomly from cycle to cycle. Synchronization and phase transitions have been studied in ensembles of such coupled oscillators [7–9].

On the other hand, in many physical or biological systems, the individual elements that compose the whole system may not be spontaneously oscillatory, but rather are excitable. In such cases, the individual elements "fire" (become excited) at random times following an external stimulus, and summate to produce the macroscopic dynamics of the whole system. For example, whereas isolated cortical neurons fire very irregularly in response to a depolarizing, constant current stimulus [10,11], *in situ* in the brain the integrated behavior of neuronal spikes is reliable and precise, forming spatiotemporal patterns. Within muscle cells, the elementary events underlying excitation-contraction coupling are calcium sparks [12,13], caused by the random excitation in time and space of subcellular calcium release units (CRUs). These microscopic events summate to give rise to highly reproducible macroscopic whole-cell calcium dynamics. For example, calcium alternans, a period-2 behavior of the whole cell, has been widely observed in cardiac muscle [14,15] and has been linked to lethal cardiac arrhythmias [16]. Yet the underlying mechanisms are not completely understood.

In this Letter, we investigate the macroscopic dynamics of a system of locally coupled excitable elements (such as the CRUs in a cardiac cell) subjected to external periodic forcing (e.g., cardiac pacemaking). We use the three-state oscillator model by Prager *et al.* [6] with modifications to describe the random excitation and refractoriness of the excitable elements. We show that a macroscopic period-2 behavior emerges via a period-doubling bifurcation due to the interactions of the randomly firing elements at the microscopic level.

A model of coupled randomly excitable elements.— The excitable element is modeled by a three-state cycle [Fig. 1(a)] similar to the one developed by Prager *et al.* [6]: $A \rightarrow B \rightarrow C \rightarrow A$. In state A, the element is fully recovered from any previous excitation, and is available to transit to state B with rate constant p. State B is the excited state with a fixed dwell time $\tau_B = 20$ in this study. State C is the refractory state with dwell time (refractory period)

$$\tau_C = T_0[1 + \sigma + (1 - \sigma)\xi], \tag{1}$$

where ξ is a uniform random number between 0 and 1, and σ ($|\sigma| \leq 1$) determines the variability of the refractory

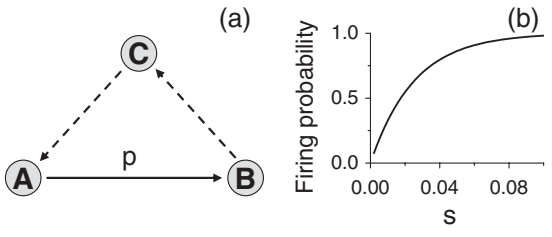

FIG. 1. (a) A schematic plot of the three-state model. See text for details. (b) The firing probability versus stimulus strength s. $T_0 = 150$ and $\delta = 0.025$.

period. In Eq. (1), when $\sigma = 1$, the refractory period is fixed, i.e., $\tau_C = 2T_0$. Otherwise, the refractory period is random with a minimum value $\tau_{C\,\min} = T_0(1 + \sigma)$. Therefore, as σ decreases, the refractory period decreases, but its variance increases. Denoting the excitation status of an element as u, we map the excited state B to $u = 1$ and all other states to $u = 0$. The rate constant p is set to $p = se^{-\delta(t \bmod T)}$ with driving period T and stimulus strength s [17]. The firing probability for an isolated element as a function of the stimulus strength s is shown in Fig. 1(b), which saturates at large s as expected.

In a two-dimensional array, the excitable elements are coupled to their nearest neighbors by modifying p to

$$p(i, j) = se^{-\delta(t \bmod T)} + \rho \frac{c(i, j)^k}{c(i, j)^k + (c_0)^k}, \qquad (2)$$

where $c(i, j) = u(i - 1, j) + u(i + 1, j) + u(i, j - 1) + u(i, j + 1)$ counts the number of excited neighbors. All elements in the array are subjected to the same periodic forcing. The default parameter set used in this study, if not explicitly stated, is: $T_0 = 150$, $s = 0.012$, $\delta = 0.025$, $\rho = 1$, $\sigma = 0.1$, $c_0 = 1.5$, and $k = 10$ [18]. We summarize the state of the whole system with the macroscopic variable

$$x(t) = \frac{1}{N_0} \sum_{i,j} u(i, j; t), \qquad (3)$$

where $N_0 = N^2$ is the total number of elements in the array.

The stochastic transition from state A to state B is simulated using the methods of Gillespie [19] and Clay and DeFelice [20] with a time step of $dt = 0.001$. Specifically, after an excitable element transitions to state A from C, a random dwell time τ_A is chosen using $\ln\xi = -\int_0^{\tau_A} p(t)dt$, where ξ is a random number uniformly distributed in (0,1] generated at the moment of transition. After staying at A for duration τ_A, the element transitions to B. The dwell time in state B is fixed; the dwell time in state C is also random, but chosen by the simpler method of Eq. (1).

Numerical simulation.—In a simulation of a 200×200 array of coupled randomly excitable elements, the whole system is almost periodic (period 1) with small fluctuations when the driving period T is long [Fig. 2(a)]. If the system is driven at a higher frequency, a period-2 behavior emerges in the beat-to-beat alternation of the macroscopic variable [Fig. 2(b)]. However, for both cases, the individual elements do not themselves exhibit periodic behavior, but rather fire randomly (Fig. 2). As shown in the snapshots in Fig. 2(c), the spatial pattern of the random firing is unique at each beat. (Note the lack of complete uniformity, with random clusters forming.)

As T decreases, the state of the system bifurcates from period 1 to period 2 and then reverses back to period 1 [Fig. 3(a)]. The range of T in which the period-2 behavior occurs depends on the coupling strength ρ between neighboring elements [Figs. 3(b) and 3(c)]. As ρ increases, period 2 occurs in a narrower range of higher driving rates.

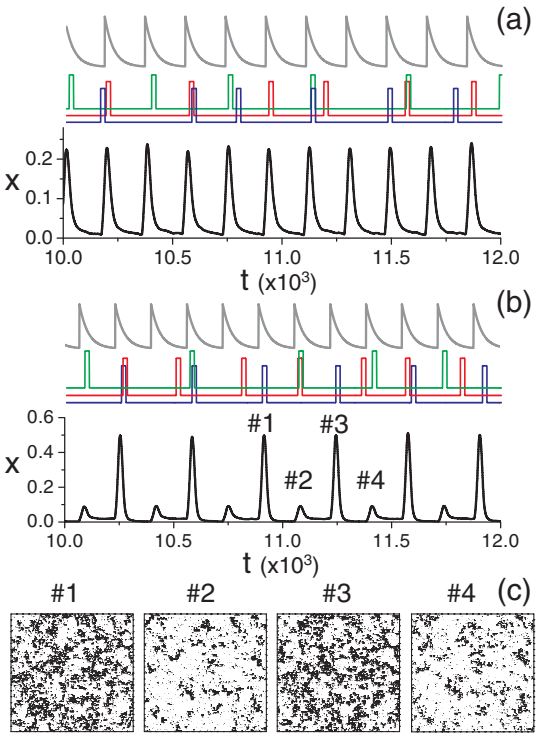

FIG. 2 (color online). (a) Shown are the stimulus [$se^{-\delta(t \bmod T)}$, top], three example traces (u) of individual elements (middle), and the macroscopic state variable x (bottom) vs time for $T = 185$. (b) Same as (a) but for $T = 165$. (c) Snapshots of spatial array taken at the peaks of four consecutive beats (marked as #1, #2, #3, and #4) for $T = 165$. The black pixels are for $u = 1$ and white for $u = 0$.

The dependence of the period-2 behavior on the stimulus strength s is shown in Fig. 3(d) and 3(e). If the external stimulus is either too weak or too strong, no period-2 behavior is observed [Fig. 3(d)]. Note that the period-2 behavior occurs over a much wider range of coupling strength ρ for smaller stimulus strength s [Fig. 3(e)]. In other words, for high cooperativity, period-2 behavior tends to occur at low stimulus strength. In this case, the excited elements are sparsely distributed. Because of strong coupling, an excited element can easily recruit its neighbor to fire, which can lead to a sequential firing cascade and thus localized wave propagation in the array. [The dashed lines in Figs. 3(b) and 3(e) mark the critical coupling strength above which a planar wave starting at one end can propagate throughout the whole array.] This is similar to experimental observations in cardiac myocytes in which local calcium-induced calcium waves are involved in the genesis of whole-cell calcium alternans [14,21]. More generally, this analysis links alternans dynamics to wave dynamics in networks of coupled excitable elements.

Besides excitability, refractoriness also plays an important role in the genesis of period-2 behavior. In Fig. 3(f), we show x versus σ for $T = 160$. The bifurcation occurs when σ is close to -0.1 (or $\tau_{C\,\min}$ close to 135). As σ

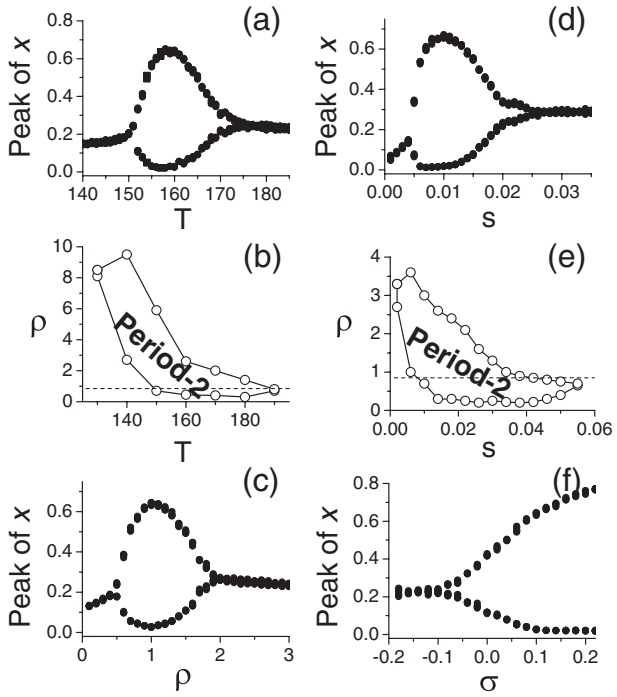

FIG. 3. (a) Peak of x vs T. (b) Period-2 region in the $\rho - T$ space. (c) Peak of x vs ρ for $T = 160$. (d) Peak of x versus the stimulus strength s for $T = 160$. (e) Period-2 region in the $\rho - s$ space for $T = 160$. (f) Peak of x vs σ for $T = 160$.

increases to 0.1, x becomes very low in one cycle, and high in the next cycle, indicating that the refractory period is so long that most of the elements fire every other cycle.

A mean-field representation.—To understand how the microscopic events interact collectively to create the macroscopic dynamics, we formulated a discrete-time mean-field representation of the macroscopic state variable x. Assume that during a cycle, α is the probability of an element being excited by an external stimulus (a primary event); γ is the probability of being excited by an excited neighbor due to coupling (a secondary event); and β is the probability of an excited element remaining in the refractory state during the next beat. If, for the kth beat, N_k out of N_0 total elements are excited, then for the $(k+1)$th beat, $N_a = N_0 - \beta N_k$ elements are available for excitation, and the number of primary excitation events for the $(k+1)$th beat is αN_a. The number of secondary events is a fraction f of the remaining available elements, i.e., $(1-\alpha)N_a f$. Therefore, the total number of excited elements at the $(k+1)$th beat is

$$N_{k+1} = \alpha N_a + (1-\alpha)N_a f = (N_0 - \beta N_k)[\alpha + (1-\alpha)f]. \quad (4)$$

The task now is to determine f and its dependence on N_k and the other parameters. The specific form of f also depends on how the elements are coupled. Here, we propose an explicit form of f for a 2D array with four-nearest-neighbor coupling. For simplicity, we also assume that a recruited element cannot further recruit its own neighboring elements. The derived function f is (see [22] for detailed explanation)

$$f(N_k) = 1 - [1 - \alpha\gamma(1 - \beta N_k/N_0)]^4. \quad (5)$$

Combining Eqs. (4) and (5), one can obtain the steady state of the system [Fig. 4(a)] and study its stability. Linearizing Eq. (4) at its steady state, one obtains the eigenvalue as

$$\lambda = -\alpha\beta - (1-\alpha)\beta[f(N_s) + (N_0 - \beta N_s)f'], \quad (6)$$

where N_s is the steady state and $f' = df/dN_k$. The condition for the steady state to become unstable leading to period-doubling is $\lambda < -1$. A bifurcation diagram [Fig. 4(a)], and a phase diagram [Fig. 4(b)] obtained by iterating Eq. (4) demonstrates that period-2 behavior occurs at a combination of intermediate primary excitation rate α, high cooperativity γ, and large β (equivalent to long refractory period), agreeing with the numerical simulation.

To determine whether the mechanism of period-doubling in the mean-field representation agrees with the

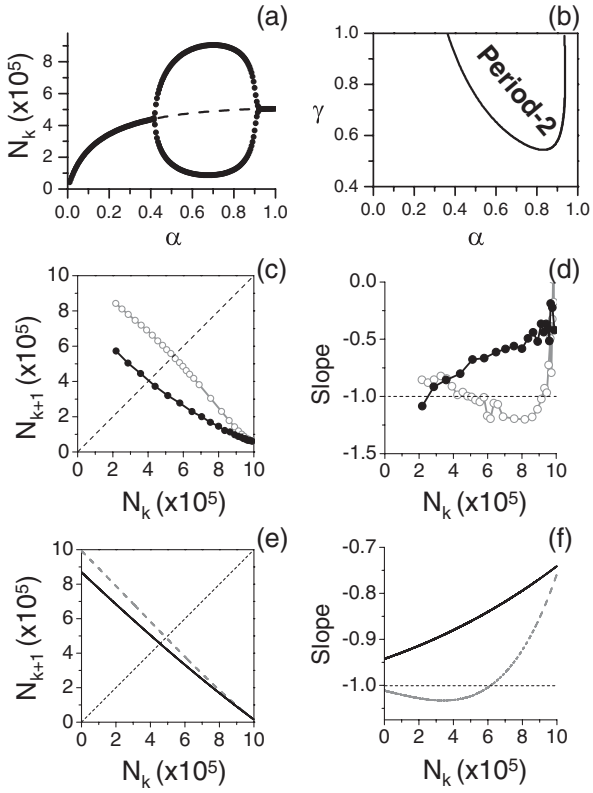

FIG. 4. (a) Number of excited elements vs α using Eq. (4). $N_0 = 10^6$, $\beta = 0.98$, and $\gamma = 0.9$. Dashed line is the unstable fixed point. (b) The period-2 region in γ-α parameter space for $\beta = 0.98$. (c) First-return map calculated from the coupled (1000×1000) array for $\rho = 1$ (open circles) and $\rho = 0.2$ (closed circles). (d) The slopes of the two curves in (c). (e) Plot of Eq. (4) for $\gamma = 0.8$ (dashed line) and $\gamma = 0.2$ (solid line). $\alpha = 0.75$ and $\beta = 0.98$. (f) The slopes of the two curves in (e).

mechanism of period-doubling in the coupled excitable elements, we calculate the first-return map of the simulated coupled system and compare it with the theoretical equation [Eq. (4)]. We generate the map as follows. Initially, all the elements are in state A. We deliver two stimuli of period T and measure the number of excited elements during both the first stimulus (N_k) and the second stimulus (N_{k+1}). We vary s for the first stimulus so that N_k varies, but fix $s = 0.012$ for the second one. Setting $T = 160$, we plot N_{k+1} vs N_k for two different coupling strengths ρ [Fig. 4(c)], one causing period 2 ($\rho = 1$) and the other not ($\rho = 0.2$). The slope of the first-return map is between -1 and 0 for $\rho = 0.2$ [Fig. 4(d)]. For $\rho = 1$, the slope decreases below -1 and then increases. This same feature also exists in the theoretical iterated map Eq. (4) as shown in Figs. 4(e) and 4(f).

Conclusions and discussion.—In this study, we use both numerical simulation and a mean-field representation to show that a period-doubling bifurcation can occur in a system of coupled stochastically excitable elements subject to global periodic forcing. The required factors underlying this bifurcation mechanism are the randomness of firing, the refractory period, and the recruitment of neighboring elements (spatial cooperativity). Note that although the refractory period and the cooperativity were explicitly varied to demonstrate their roles in the bifurcation, the randomness factor was not explicitly tested. However, it is straightforward to understand that randomness plays a crucial role in the genesis of this bifurcation, by the following reasoning. Random excitation results in a spatially random distribution of excited elements. For a high excitation rate in the previous cycle, the excitation rate will be low in the next cycle, since most of the elements which were excited in the previous cycle are still refractory. Therefore, the elements available to become excited are not only very low in number, but also randomly and sparsely distributed among a large number of refractory elements. Since the probability of two available elements being nearest neighbors is therefore low, the secondary excitation rate due to recruitment is low (small f). Conversely, if the excitation rate in the previous cycle is low, then most of the elements will be recovered and available for excitation in the next cycle. The chance of two available elements being nearest neighbors is high, and thus the secondary excitation rate is also high (large f). Therefore, due to the interaction of refractoriness and random excitation, a nonlinear function f emerges, which is key for the instability. This instability cannot occur if the recovered elements are not randomly distributed. If one assumes that the recovered elements are in a single patch of the spatial domain instead of randomly distributed among nonrecovered ones, then no matter what N_a is, f is constant [e.g., for a 2D array, one can analytically derive $f = 1 - (1 - \alpha\gamma)^4$]. Since $f \leq 1$, then according to Eq. (6), $|\lambda| = \beta[\alpha + (1 - \alpha)f] < 1$, and no instability can occur.

Finally, we would like to point out the model studied here may be widely applicable to many systems, especially biological systems composed of thousands of randomly excitable elements, such as the cells in neural tissue and muscle. In heart cells, this work forms a theoretical foundation for understanding how the subcellular spatial organization of CRUs leads to collective behaviors such as calcium alternans and calcium waves due to the interaction between the ''three R's'': Random firing, Refractoriness, and Recruitment of CRUs.

This work is supported by NIH/NHLBI P01 HL078931, a grant from the China Scholarship Council (X. C.), and the Laubisch and Kawata Endowments.

*Correspondence to: zqu@mednet.ucla.edu.

[1] A. T. Winfree, J. Theor. Biol. **16**, 15 (1967).
[2] P. C. Matthews and S. H. Strogatz, Phys. Rev. Lett. **65**, 1701 (1990).
[3] S. H. Strogatz and I. Stewart, Sci. Am. **269**, 102 (1993).
[4] Y. Kuramoto, *Chemical Oscillations, Waves, and Turbulence* (Springer, New York, 1984).
[5] J. A. Acebron *et al.*, Rev. Mod. Phys. **77**, 137 (2005).
[6] T. Prager, B. Naundorf, and L. Schimansky-Geier, Physica A (Amsterdam) **325**, 176 (2003).
[7] K. Wood *et al.*, Phys. Rev. E **74**, 031113 (2006).
[8] K. Wood *et al.*, Phys. Rev. Lett. **96**, 145701 (2006).
[9] B. Fernandez and L. S. Tsimring, Phys. Rev. Lett. **100**, 165705 (2008).
[10] P. Tiesinga, J. M. Fellous, and T. J. Sejnowski, Nat. Rev. Neurosci. **9**, 97 (2008).
[11] B. Englitz, K. M. Stiefel, and T. J. Sejnowski, Neural Comput. **20**, 44 (2008).
[12] H. Cheng, W. J. Lederer, and M. B. Cannell, Science **262**, 740 (1993).
[13] X. Wang *et al.*, Nat. Cell Biol. **7**, 525 (2005).
[14] M. E. Diaz, D. A. Eisner, and S. C. O'Neill, Circ. Res. **91**, 585 (2002).
[15] E. Picht *et al.*, Circ. Res. **99**, 740 (2006).
[16] J. N. Weiss *et al.*, Circ. Res. **98**, 1244 (2006).
[17] In neural or cardiac cells, the action potential has a very fast upstroke followed by a slow (more or less exponentially) decaying phase. Therefore, if one considers the subcellular organelles as random excitable elements, they are subjected to an external force similar to the one in this study. However, the phenomena shown in this study occur not only with the stimulus waveform used here, but also for other stimulus waveforms such as pulsatile or sinusoidal waveform.
[18] $k = 10$ gives rise to a very steep Hill function in Eq. (2), yet it is reasonable since excitable elements generally exhibit an ''all-or-none'' response. Period-2 behavior can occur for smaller k but in narrower parameter ranges.
[19] D. T. Gillespie, J. Phys. Chem. **81**, 2340 (1977).
[20] J. R. Clay and L. J. DeFelice, Biophys. J. **42**, 151 (1983).
[21] D. A. Eisner *et al.*, Cell Calcium **35**, 583 (2004).
[22] For the derivation of Eq. (5), see EPAPS Document No. E-PRLTAO-103-063931. For more information on EPAPS, see http://www.aip.org/ pubservs/epaps.html.